March 6, 2006

Spontaneous Formation of Stable Aligned Wrinkling Patterns

Edwin P. Chan
Alfred Crosby, *University of Massachusetts - Amherst*

Spontaneous formation of stable aligned wrinkling patterns

Edwin P. Chan and Alfred J. Crosby*

Received 3rd November 2005, Accepted 19th February 2006
First published as an Advance Article on the web 6th March 2006
DOI: 10.1039/b515628a

We introduce a new methodology to produce aligned, or patterned, surface wrinkles on a soft elastomer sans topography. The surface buckles orient through the manipulation of the local stress distributions, which we control by defining specific regions of local differences in the elastic moduli of the material.

Surface buckling, or wrinkling, can be generated in a variety of systems that include: (1) thermally or mechanically stressed metallic,[1,2] polymeric[3,4] and silicate[5–7] thin films supported on elastomeric substrates, (2) dried thin films prepared by the sol-gel method,[8,9] as well as (3) soft gels placed under geometric confinement that are swollen[10] or dried.[11] These surface relief structures are interesting for their pattern complexity as well as ease of formation with a dominant periodicity. In this report, we demonstrate the spontaneous alignment of surface wrinkles through pre-defined regions of local moduli-mismatch combined with osmotic pressure. The moduli-mismatch is produced by converting selective areas of a poly(dimethyl siloxane) (PDMS) elastomer surface into a silicate thin surface layer through a UV–Ozone (UVO) oxidation process.[12–15] Geometric confinement of the oxidized regions coupled with an osmotic stress leads to the alignment of the surface wrinkles. The osmotic stress is induced by swelling the elastomer with a photopolymerizable *n*-butyl acrylate (*n*BA) monomer, thus allowing the aligned wrinkles to be stabilized upon ultraviolet (UV) exposure. The shape of oxidized regions controls the local stress state upon swelling which in turn directs and orients the formation of these wrinkles. This approach is amenable to creating relief patterns on a variety of polymer systems to yield devices that can potentially function as diffraction gratings,[6] smart adhesives,[16] mechanical strain sensors,[4] microfluidic devices[17] as well as cell culture surfaces.[18,19]

To generate a film with local moduli-mismatch regions, we UVO oxidize a PDMS elastomer selectively by masking regions with either a copper grid or a thin photoresist layer. The top layer of the exposed regions of the elastomer is converted into a silicate thin film which becomes stiffer and less elastomeric compared with the unmodified PDMS.[5] At this stage, no cracks develop on the silicate surface layer. The entire sample is then coated with a photopolymerizable *n*BA monomer solution that swells the elastomer, but only causes the wrinkling patterns to form in the oxidized regions—where a local moduli-mismatch of the PDMS exists. Upon photopolymerization with UV, the aligned wrinkling pattern is stabilized and the poly(*n*-butyl acrylate) (p*n*BA) coating is removed to reveal a highly textured, oriented pattern on the PDMS surface (Fig. 1). As revealed by the SEM micrograph, the aligned wrinkling pattern consists of grooves or cusps that form on the surface (Fig. 1b). While the length of the grooves varies from 30 to 300 μm, the periodicity between neighboring grooves remains uniform at approximately 30 μm. These self-assembled textured patterns can also be made to span large areas (Fig. 1c). For this sample, we oxidized a 20 cm^2 PDMS surface to produce wrinkling patterns that spanned the entire area. These patterns do not resemble the "spider-web" formation of Fig. 1a, but an intricate, intertwined, zipper-pattern develops in this case. Although no attempts were made to induce orientation, local registry of these zipper patterns (Fig. 1c insert) is observed. The mechanism responsible for local registry of the zipper patterns is yet to be determined; however, the generation of the zipper pattern is very reproducible and is observed for multiple samples produced in the same manner. We orient the surface buckles by geometrically controlling the moduli-mismatch regions. This is done by oxidizing alternating striped regions of a PDMS film (Fig. 2). As Fig. 2b illustrates, the alignment of surface buckles is very sensitive to the shape of the local-moduli mismatch regions. At the center of this "starburst" pattern (Fig. 2a), the surface buckles are randomly oriented since the geometric constraint is not biased. However, by confining the formation of the surface buckles within the oxidized

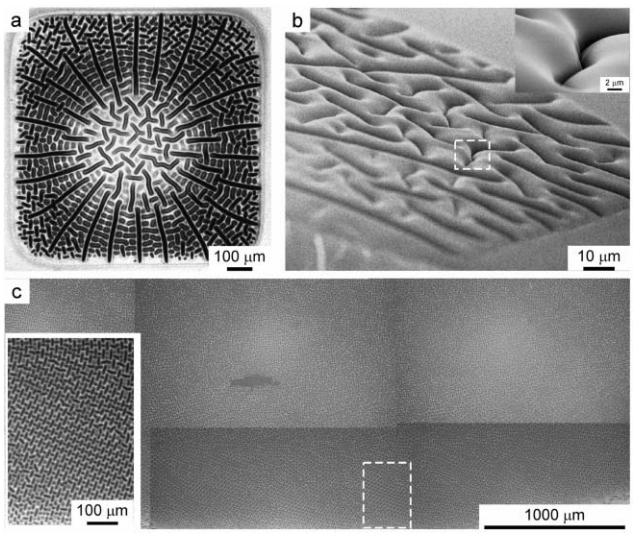

Fig. 1 (a) Radial buckling pattern formed on a PDMS film that has been selectively oxidized. (b) SEM micrograph of the buckled surface taken from the radial pattern. The insert shows that cusps are formed by the p*n*BA film which is believed to interdigitate with the underlying PDMS. (c) For a PDMS film (76 mm × 25 mm) where the entire surface is oxidized, the buckling patterns span the entire surface. Certain areas of the film show alignment of very intricate patterns that resemble zippers.

Polymer Science and Engineering, University of Massachusetts, Amherst, MA, USA. E-mail: epc@mail.pse.umass.edu; crosby@mail.pse.umass.edu; Fax: (413)545 0082; Tel: (413) 577 1313

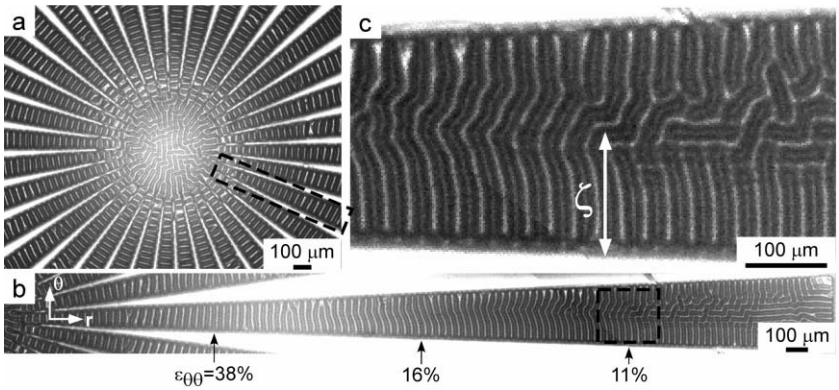

Fig. 2 (a) Alignment of surface buckles using stripes of UVO lines to generate the "star-burst" pattern. (b) Within a UVO stripe, the surface buckles orient perpendicular to the radial direction. The ordered wrinkles persist over a persistence length ζ, which scales with the azimuthal strain $\varepsilon\theta\theta$ and the modulus mismatch ratio. The azimuthal strain is calculated by comparing the change in width of the stripe before and after exposing the PDMS to acrylate solution. The highlighted region shows the onset of disorder wrinkles. (c) ζ is determined from this region where disorder begins to occur.

strip (Fig. 2b), alignment is clearly observed. The orientation of the wrinkles persists over a finite length ζ beyond which the wrinkles become disordered. This persistence length is dependent on the azimuthal strain ($\varepsilon\theta\theta$) of the local region and the modulus-mismatch ratio.[20] Based on an estimated strain of 11% (determined by the change in width prior to monomer swelling and after the buckle formation) and a calculated modulus-mistmatch ratio, we calculate $\zeta \sim 170$ μm, which is comparable to the measured value of 155 μm obtained from Fig. 2c.

The buckling patterns formed are a type of elastic instability that arise by buckling of the laterally confined swollen PDMS layer. Our approach builds upon the observations of Tanaka *et al*[10] for swollen gels and the surface wrinkling patterns reported by Bowden *et al*[1] on the buckling of a metallic thin film on a PDMS elastomer. Tanaka and coworkers have demonstrated that osmotic force can cause surface wrinkling patterns on a polyacrylamide gel, however, the generated patterns are stable only when adhered to a rigid substrate and the wrinkles would coalesce and disappear when the gel becomes free-standing.[10] Moreover, their buckling patterns were isotropic as the buckling stress was equi-biaxial. A more robust method to generating stabilized wrinkles was reported by Bowden and coworkers for buckling of a metallic thin film on a PDMS elastomer based on thermal expansion differences between the two materials.[1] Although they successfully demonstrated the generation of stable, oriented wrinkling patterns, it required the use of a topographically patterned PDMS elastomer in order to attain alignment. Our method offers several advantages over these previous approaches: (1) stability of the wrinkles is achieved by the photopolymerization of the *n*BA monomer, (2) alignment of the surface wrinkles is not controlled by a pre-defined topographic pattern and (3) versatility of the approach in generating a large patterned area as the buckling stress is not dependent on a mechanical nor thermal bias.

For our process, the surface buckles in the following manner (Fig. 3). The UVO oxidation converts the top surface of the PDMS into a silicate thin film whose thickness is of the order of 100 nm[13,14] and creates the necessary local moduli difference in the material. At this point, no surface wrinkles are observed. The PDMS surface is then coated with an *n*BA solution. The PDMS layer directly beneath the silicate swells in the presence of the monomer solution. If the silicate layer is absent, the PDMS is free to expand and wrinkling is not observed. However, for regions where a rigid silicate layer is present (insert in Fig. 3), the expansion of the swollen PDMS becomes laterally confined. Consequently, the swollen PDMS layer experiences competing forces of osmotic pressure (acrylate monomer uptake) *versus* geometric confinement (as the silicate swells significantly less than the PDMS) and is forced into a complex state of stress. The specific stress distribution is defined by the convolution of the osmotic pressure and the boundary conditions imposed by the shape of the oxidized region. As the silicate layer is covalently bound to the PDMS top layer, strain compatibility boundary conditions must be satisfied at this interface (Fig. 3B). At a critical degree of swelling, this imposed compressive stress at the silicate–PDMS interface causes both the PDMS and the silicate to buckle (Fig. 3C). The buckling process, similar to the previous work on buckling of thin rigid films,[1–6,20] is essentially a variation of the classic Euler buckling of a rigid rod under compression[21] except in our system the buckling of the PDMS top layer occurs two dimensionally. Besides serving as a swelling agent, the photo-curable acrylate solution helps to stabilize the wrinkling patterns. Since the *n*BA solution diffuses into the PDMS prior to the photopolymerization step, the p*n*BA polymer chains interdigitate with the PDMS elastomer after the photopolymerization step. This interdigitation helps to lock the surface wrinkling patterns.

Prior to photopolymerization, a glass superstrate is placed on top of the acrylate solution. Without removal of the glass superstrate, the wrinkling pattern is not observed as there is insufficient optical contrast to observe the patterns. Upon removal, the p*n*BA film fractures in a cohesive manner. The cohesive fracture follows the contour of the surface wrinkling structures due to the extreme mismatch in the near-interfacial moduli.

To demonstrate confirmation of the buckling process, we control the wavelength of the surface wrinkles (Fig. 4). For a thin film adhered to an elastomeric support, the buckling wavelength (λ) is predicted to scale proportional to the thickness (h_p) of the thin film according to the following equation:[22]

$$\lambda = 2\pi h_p \left[\frac{E_p^*}{4E_m}\right]^{1/3} \quad (1)$$

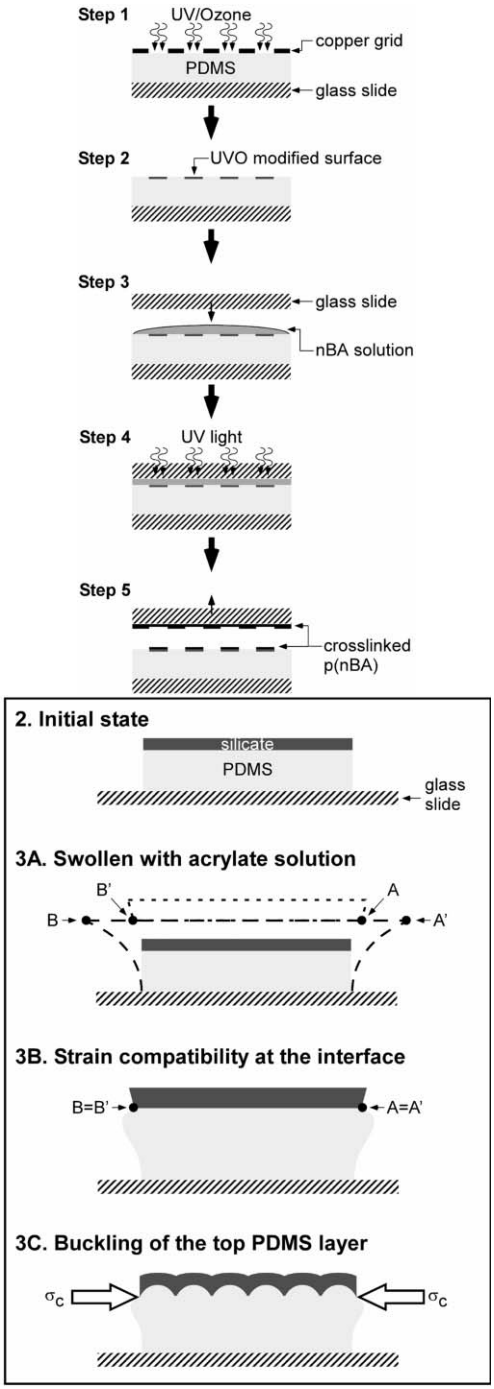

Fig. 3 Top: procedure for creating the oriented wrinkling pattern. (1) A PDMS elastomer is selectively UVO oxidized by masking the surface with a copper grid, (2) which oxidizes the surface to convert into a silicate layer. (3) Acrylate solution is deposited onto this newly oxidized surface, (4) covered with a glass superstrate and irradiated with UV. (5) Separation of the glass superstrate reveals the wrinkles on the oxidized regions. Bottom insert: buckling process after the PDMS is swollen by the *n*BA solution. (3A) The acrylate monomer swells both the PDMS and silicate layers but the softer PDMS wants to expand to a greater extent compared with the silicate as depicted hypothetically by points A and A′ (or similarily B and B′). (3B) Since the PDMS is covalently bound to the stiff silicate layer, expansion of PDMS at and near the PDMS–silicate interface is laterally confined. Strain compatibility boundary conditions at the interface require that A = A′ and B = B′. (3C) This lateral confinement places the swollen PDMS into a compressive stress state σ_c. At a critical σ_c, the swollen PDMS buckles which in turn buckles the silicate layer.

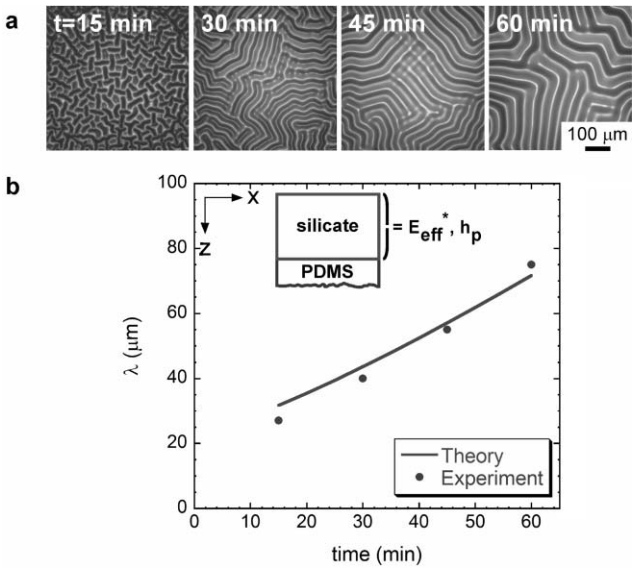

Fig. 4 (a) Wavelength dependence of the buckling patterns with respect to UVO oxidation times. The wavelength (λ) increases with oxidation times (t), λ = 27, 40, 55, and 75 μm respectively. A single PDMS film (thickness = 88 μm), is used to generate this gradient. Sections of the film are oxidized in increments of 15 min. Afterwards, the entire film is coated with *n*BA solution followed by photopolymerization. (b) Scaling relationship of buckling wavelength, λ *versus* oxidation time. Although the UVO oxidation creates a multilayer silicate film with different elastic modulus and thickness values, we replaced them with an effective modulus, E_{eff}* and total layer thickness, h_p. The solid curve shows the theoretical prediction for λ by using the experimental results from Efimenko *et al* for the UVO oxidation of PDMS films.

where $E_p^* = E_p/(1-\nu_p^2)$ is the reduced Young's modulus of the thin film (ν_p is the Poisson's ratio) and E_m is the Young's modulus of the unmodified PDMS. The simplified form of the equation assumes that $\nu_m = 0.5$, we refer the reader to ref. 20 for the full equation. Based on eqn (1), for a 100 nm thick silica layer with ν_p = 0.33 and E_p = 50 GPa, E_m = 1 MPa, we obtain a $\lambda \sim 15$ μm, which is much lower than the experimentally observed wavelength of 27 μm. While this model accurately predicts the buckling wavelength for a bi-layer system consisting of a thin film on an elastic support,[1–4] our system is more complicated than this. The UVO oxidation process creates a film with properties changing as a function of depth beneath the surface. According to Efimenko *et al*, the UVO process oxidizes the PDMS and converts the top surface into a dense silicate layer with a thickness of 5 nm.[13] The thickness of this top layer is virtually unchanged for oxidation times beyond 10 min, but the ozone diffusion beneath this dense layer becomes rate-limiting and results in an intermediate diffuse silicate layer with a varying silica density. The thickness of the intermediate layer varies depending on the oxidation conditions and time and can reach as high as 160 nm.[14] Beneath the diffuse layer is the neat PDMS where the UVO process has not chemically altered the composition.

The buckling wavelength increases as a consequence of the greater stiffness of the combined dense silicate and intermediate layer, which increases the lateral confinement experienced by the swollen PDMS layer. With increasing oxidation time, the overall silicate layer thickness increases, thus indirectly causing an increase

in the buckling wavelength. Shown in Fig. 4a is the wrinkling pattern for a PDMS film with separate regions that are UVO treated for different times. The wavelength of the pattern increases from 27 μm up to 75 μm as we vary oxidation time from 15 min to 1 h (in 15 min increments).

Based on the above model for our silicate layer, we rework the buckling model by assuming that the modulus of the silicate layer varies as a function of depth, z. As a first order approximation, we define an effective modulus for this "composite" film:

$$E^*_{\text{eff}} = \frac{\int_0^{h_p} E^*(z)\cdot z^2\, dz}{\int_0^{h_p} z^2\, dz} \qquad (2)$$

We can substitute E_p* with E_{eff}* in eqn (1). The effective modulus, E_{eff}* is dependent on the conversion percentage of PDMS-to-silicate, $\phi(z)$ and is related to the reduced Young's modulus of pure silica, E_{silica}* by the following expression:

$$E^*_{\text{eff}} = \phi(z)\cdot E^*_{\text{silica}} \qquad (3)$$

For time scales relevant to our process, both the parameters $\phi(z)$ and the total silicate layer thickness, h_p scale proportionally with the UVO oxidation times. We use the experimental results of Efimenko and coworkers on the UVO oxidation of PDMS films[13] to derive empirical relationships for both $\phi(z)$ and h_p as a function of time. This allows us to derive the scaling relationship for the buckling wavelength *versus* oxidation time, a plot of this expression along with our experimental results is shown in Fig. 4b. We are able to fit the predicted curve with the experimental results quite nicely by assuming E_{silica}* = 100 GPa, which is a reasonable value for pure silica.

When a semi-infinite (in lateral dimensions) PDMS film is oxidized, the swollen PDMS layer experiences an equi-biaxial compression due to lateral confinement by the silicate layer. The PDMS swollen layer buckles randomly as there is a lack of driving force for the surface buckles to orient. However, if the dimensions of the oxidized PDMS are defined and finite, the boundary conditions dictate the stress distribution within the region of higher moduli. This boundary-imposed stress distribution leads to the radial wrinkling pattern for the square oxidized regions (Fig. 1a) and is more conclusively illustrated by the "starburst" pattern (Fig. 2).

For both examples, the wrinkles orient perpendicular to the edge as defined by the boundary between the soft (unconfined PDMS) and hard (confined PDMS due to the silicate layer) regions. At the edge of this soft–hard PDMS boundary, a greater compressive stress is experienced parallel to the edge compared with normal to the edge. As a consequence, the buckles orient perpendicular to the radial direction. This control of the primary stress direction is dictated by the traction conditions parallel and perpendicular to the defined boundaries. Analogous control is described by Huck *et al.* with topographical, non-compositional patterns.[2] For the stripe regions of the "starburst" pattern, this greater compressive stress parallel to the edge causes the wrinkles to be oriented perpendicular to the radial direction (Fig. 2b). At the center of the "starburst", the patterns form randomly since the soft–hard PDMS boundaries are absent (Fig. 2a). In the case of the radial pattern (Fig. 1a), the primary buckles orient orthogonal to the edge of the overall square oxidized region. Subsequently, secondary patterns or spokes perpendicular to the radial buckles form as a result of the new boundary conditions established by the primary radial buckles. It is interesting to note that this form of hierarchical wrinkling patterns has not been previously reported and could have potential as an alternative method for generating a hierarchical self-assembled pattern.

In summary, our approach to pattern generation is unique for the spontaneity of relief structure formation and simplicity in attaining pattern alignment. The alignment of the surface patterns is achieved without the aid of a topographic elastomer, rather, we form oriented patterns by confining the buckling regions with local moduli differences. In general, the process is amenable to a wide range of polymers—different photopolymerizable swelling agents, different elastomers, and different moduli convergence schemes. Although we only demonstrated the wrinkling pattern in a planar configuration, the general process is amenable to patterning nonplanar surfaces. Through clever control of the local stress state of the film—simply by selective oxidization of the PDMS, it is possible to fabricate oriented and even more complex buckling patterns. Such patterns may find potential application as: (1) a smart adhesive—the acrylate formulation can be adjusted to yield a soft elastomer, the presence of these surface patterns may yield drastic changes in the adhesive properties of the elastomer,[16] and (2) a new patterning technique—this approach may also be applicable for rapid patterning of a large surface; simply adhere the *n*BA coated UVO-PDMS slab onto any arbitrary surface, cure with UV and then separate to pattern the previously smooth surface.

Experimental

(a) Buckling process by swelling with acrylate formulation: the photocurable acrylate formulation consists of *n*-butyl acrylate monomer (75 wt%), ethylene glycol dimethacrylate crosslinker (25 wt%), (Sigma-Aldrich) and commercial photoinitiators Irgacure® 814 and 719. The monomer and crosslinker are purified by filtering through alumina to remove the inhibitors and then combined with the photoinitiators to yield a clear bright yellow liquid. Crosslinked PDMS films are prepared by combining Dow Corning Sylgard 184 oligmer with catalyst (10 : 1 by weight), casting on glass substrates and cured at 110 °C for 1 h. The thickness of the PDMS films is 1 mm for the samples in Fig. 1, 2 and 0.65 mm for the PDMS film in Fig. 4. This solution is deposited onto the UVO-PDMS surface and covered with a glass superstrate to spread the solution uniformly across the PDMS surface. The entire assembly is irradiated with UV (OAI 500 W DUV, λ = 365 nm, intensity = 20 MW cm^{-2}) for 6 min to photopolymerize and crosslink the acrylate mixture. Finally, the superstrate is removed by mechanical peeling to reveal the wrinkling pattern on the PDMS surface.

(b) Spider-web pattern: a copper grid is placed above the crosslinked PDMS film and is then UVO oxidized for 15 min. The copper grid (square array with 1 mm by 1 mm squares) serves as a mask to allow for selective surface chemical modification.

(c) Starburst pattern: we substitute the copper grid mask with a photoresist thin film. Shipley SPR220 photoresist (MicroChem Corp.) is spin-coated onto a 1 mm thick PDMS film at 6000 rpm for 60 s, pre-baked at 95 °C for 60 s and then exposed with UV

(OAI 500 W DUV) for 105 s through a printed photomask containing the "starburst" pattern. The film is post-expose baked at 95 °C for 60 s and developed for 2 min which strips away the exposed resist. This photoresist coated PDMS film is then UVO oxidized for 30 min. Following cool-down, the remaining photoresist is removed by exposing with ethyl lactate and rinsing with DI water and then dried in a vacuum for 2 days until use.

(d) Global surface wrinkles with zipper patterns: the entire PDMS film is completely oxidized for 15 min without any mask.

Acknowledgements

The authors thank Dr. Ryan Hayward for insightful discussions and acknowledge NSF-MRSEC Central Facilities for use of their SEM and AFM. Funding for this work is provided by NSF CAREER Award DMR-0349078 and 3 M Non-tenured Faculty Research Award.

References

1 N. Bowden, S. Brittain, A. G. Evans, J. W. Hutchinson and G. W. Whitesides, *Nature*, 1998, **393**, 146–149.
2 W. T. S. Huck, N. Bowden, P. Onck, T. Pardoen, J. W. Hutchinson and G. W. Whitesides, *Langmuir*, 2000, **16**, 3497–3501.
3 C. Harrison, C. M. Stafford, W. Zhang and A. Karim, *Appl. Phys. Lett.*, 2004, **85**, 4016–4018.
4 C. M. Stafford, C. M. Harrison, K. L. Beers, A. Karim, E. J. Amis, M. R. Vanlandingham, H. -C. Kim, W. Volksen, R. D. Miller and E. E. Simonyi, *Nat. Mater.*, 2004, **3**, 545–550.
5 D. B. H. Chua, H. T. Ng and S. F. Y. Li, *Appl. Phys. Lett.*, 2000, **76**, 721–723.
6 N. Bowden, W. T. S. Huck, K. E. Paul and G. W. Whitesides, *Appl. Phys. Lett.*, 1999, **75**, 2557–2559.
7 K. Efimenko, M. Rackaitis, E. Manias, A. Vaziri, L. Mahadevan and J. Genzer, *Nat. Mater.*, 2005, **4**, 293–297.
8 S. J. Kwon, J. -H. Park and J. G. Park, *Phys. Rev. E: Stat. Phys., Plasmas, Fluids, Relat. Interdiscip. Top.*, 2005, **71**, 011604/011601–011604/011604.
9 R. C. Hayward, B. F. Chmelka and E. J. Kramer, *Macromolecules*, 2005, **38**, 7768–7783.
10 T. Tanaka, S. -T. Sun, Y. Hirokawa, S. Katayama, J. Kucera, Y. Hirose and T. Amiya, *Nature*, 1987, **325**, 796–798.
11 E. S. Matsuo and T. Tanaka, *Nature*, 1992, **358**, 482–484.
12 C. L. Mirley and J. T. Koberstein, *Langmuir*, 1995, **11**, 1049–1052.
13 K. Efimenko, W. E. Wallace and J. Genzer, *J. Colloid Interface Sci.*, 2002, **254**, 306–315.
14 H. Hillborg, N. Tomczak, A. Olah, H. Schonherr and G. J. Vancso, *Langmuir*, 2004, **20**, 785–794.
15 M. Ouyang, R. Yuan, R. J. Muisener, A. Boulares and J. T. Koberstein, *Chem. Mater.*, 2000, **12**, 1591–1596.
16 A. J. Crosby, M. Hageman and A. Duncan, *Langmuir*, 2005, **21**, 11738–11743.
17 S. Jeon, V. Malyarchuk, J. O. White and J. A. Rogers, *Nano Letters*, 2005, **5**, 1351–1356.
18 C. D. W. Wilkinson, A. S. G. Curtis and J. Crossan, *J. Vac. Sci. Technol., B*, 1998, **16**, 3132–3136.
19 M. Yamato, C. Konno, M. Utsumi, A. Kikuchi and T. Okano, *Biomaterials*, 2002, **23**, 561–567.
20 J. Groenewold, *Physica A*, 2001, **298**, 32–45.
21 D. O. Brush and B. O. Almroth, *Buckling of Bars, Plates, and Shells*, McGraw-Hill, New York 1975.
22 H. G. Allen, *Analysis and Design of Structural Sandwich Panels*, Pergamon Press, Oxford, 1969.

